

Nonlinear Hamiltonian Waves with Constant Frequency and Surface Waves on Vorticity Discontinuities

JOSEPH BIELLO

University of California at Davis

AND

JOHN K. HUNTER

University of California at Davis

Abstract

Waves with constant, nonzero linearized frequency form an interesting class of nondispersive waves whose properties differ from those of nondispersive hyperbolic waves. We propose an inviscid Burgers-Hilbert equation as a model equation for such waves, and give a dimensional argument to show that it models Hamiltonian surface waves with constant frequency. Using the method of multiple scales, we derive a cubically nonlinear, quasilinear, nonlocal asymptotic equation for weakly nonlinear solutions. We show that the same asymptotic equation describes surface waves on a planar discontinuity in vorticity in two-dimensional inviscid, incompressible fluid flows. Thus, the Burgers-Hilbert equation provides an effective equation for these waves. We describe the Hamiltonian structure of the Burgers-Hilbert and asymptotic equations, and show that the asymptotic equation may also be derived by means of a near-identity transformation. We derive a semi-classical approximation of the asymptotic equation, and show that spatially periodic, harmonic traveling waves are linearly and modulationally stable. Numerical solutions of the Burgers-Hilbert and asymptotic equations are in excellent agreement in the appropriate regime. In particular, the lifespan of small-amplitude smooth solutions of the Burgers-Hilbert equation is given by the cubically nonlinear timescale predicted by the asymptotic equation.

© 2000 Wiley Periodicals, Inc.

1 Introduction

The most familiar class of nondispersive waves consists of hyperbolic waves whose linearized phase speed is independent of their wavenumber [12]. A less familiar class of nondispersive waves consists of waves whose linearized frequency is nonzero and independent of their wavenumber. We call these waves *constant-frequency waves*. A weakly nonlinear nondispersive hyperbolic wave has a spatial profile that propagates and slowly distorts as a result of quadratically nonlinear, three-wave interactions. The wave-profile typically satisfies an inviscid Burgers equation. By contrast, a weakly nonlinear constant-frequency wave has a spatial profile that oscillates in time and slowly distorts as a result of cubically nonlinear,

four-wave interactions. In this paper, we introduce a model equation for nonlinear constant-frequency waves and derive an asymptotic equation for the weakly nonlinear evolution of the wave-profile. We show that the same asymptotic equation describes constant-frequency surface waves on a vorticity discontinuity in a two-dimensional, inviscid, incompressible fluid flow.

The model equation for unidirectional, constant-frequency waves is

$$(1.1) \quad u_t + \left(\frac{1}{2} u^2 \right)_x = \mathbf{H}[u].$$

In (1.1) and below, \mathbf{H} denotes the spatial Hilbert transform, which is defined by

$$\mathbf{H} \left[e^{ikx} \right] = -i(\operatorname{sgn} k) e^{ikx},$$

where sgn is the usual sign function defined in (A.1). We summarize our notation in Appendix A. Equation (1.1) is an inviscid Burgers equation for $u(x, t)$ with a lower-order, nonlocal, linear, oscillatory term. We refer to (1.1) as the inviscid Burgers-Hilbert equation or, for brevity, the Burgers-Hilbert equation. Marsden and Weinstein [10] wrote down (1.1) as a quadratic approximation for the motion of the boundary of a vortex patch but did not analyze it.

Positive wavenumber solutions of the linearized equation $u_t = \mathbf{H}[u]$ have frequency equal to 1, while negative wavenumber solutions have frequency equal to -1 . Thus, (1.1) describes a single, real-valued nonlinear wave whose linearized frequency is independent of the magnitude of the wavenumber. The frequency of a real wave is an odd function of the wavenumber, so it necessarily depends on the sign of the wavenumber.

Equation (1.1) may be written as

$$(1.2) \quad u_t + \partial_x \left[\frac{\delta \mathcal{H}}{\delta u} \right] = 0, \quad \mathcal{H}(u) = \int \left(\frac{1}{2} u |\partial_x|^{-1} u + \frac{1}{6} u^3 \right) dx,$$

where ∂_x denotes the partial derivative with respect to x and $|\partial_x| = \mathbf{H}\partial_x$ is the operator with symbol $|k|$. Thus, the Burgers-Hilbert equation is Hamiltonian with respect to the constant Hamiltonian operator $-\partial_x$.

Weakly nonlinear solutions of (1.1) have the form

$$(1.3) \quad u(x, t) \sim \psi(x, t) e^{-it} + \psi^*(x, t) e^{it},$$

where $\psi(x, t)$ is a small, complex-valued amplitude-function that varies slowly in time and contains only positive-wavenumber components, meaning that

$$(1.4) \quad \mathbf{P}\psi = \psi, \quad \mathbf{P} = \frac{1}{2} (\mathbf{I} + i\mathbf{H}).$$

Here, \mathbf{P} is the projection on to positive spatial wavenumber components. Using the method of multiple scales, we show that (1.3) is an asymptotic solution of (1.1) if $\psi(x, t)$ satisfies the following cubically nonlinear, nonlocal equation

$$(1.5) \quad \psi_t = \mathbf{P}\partial_x \left[\psi |\partial_x| n - n |\partial_x| \psi \right] \quad n = |\psi|^2.$$

This equation preserves the constraint (1.4). From (1.4), we may alternatively write $|\partial_x|\psi = -i\partial_x\psi$ in (1.5), but there is no similar identity for $|\partial_x|n$ since n contains both positive and negative wavenumber components. Equation (1.5) may be written in equivalent spectral and real forms, given in (5.6) and (5.9), respectively.

Equation (1.5) has the complex Hamiltonian form

$$(1.6) \quad \psi_t + \partial_x \left[\frac{\delta \mathcal{H}}{\delta \psi^*} \right] = 0,$$

where

$$(1.7) \quad \mathcal{H}(\psi, \psi^*) = \int \left\{ \frac{i}{4} \psi \psi^* (\psi \psi_x^* - \psi^* \psi_x) - \frac{1}{2} \psi \psi^* |\partial_x| [\psi \psi^*] \right\} dx.$$

We also derive (1.5) from (1.1) by a symplectic near-identity transformation that eliminates the cubic terms from the Hamiltonian (1.2), which are non-resonant, giving the resonant forth-order terms in the Hamiltonian (1.7).

An interesting physical example of constant-frequency waves arises in two-dimensional incompressible, inviscid fluid flows. A planar discontinuity in vorticity that separates two linear shear flows is linearly stable. This stability contrasts with the Kelvin-Helmholtz instability of a vortex-sheet, across which the tangential velocity is discontinuous. A vorticity discontinuity supports surface waves that decay exponentially in space away from the discontinuity and oscillate in time with a constant frequency that is proportional to the jump in vorticity.

Remarkably, when weakly nonlinear effects are taken into account, the complex amplitude of the displacement of the vorticity discontinuity satisfies an asymptotic equation of exactly the same form as (1.5). Thus, the Burgers-Hilbert equation, with a suitably renormalized nonlinear coefficient given in (B.4) below, captures the resonant cubically nonlinear dynamics of the vorticity discontinuity. This apparent coincidence is explained, in part, by dimensional analysis, which shows that (1.1) is an appropriate model equation for constant-frequency *surface* waves.

A planar vorticity discontinuity provides a local approximation of a smooth vortex patch near its boundary, so the asymptotic equation (1.5) is relevant to the dynamics of vortex patches [3, 9, 11]. A spectral form of an equation related to (1.5) was derived by Dritschel [5] for the motion of a circular vortex patch.

Numerical computations show that smooth solutions of (1.5) typically develop singularities in finite time, in which the derivative ψ_x blows up. This singularity formation corresponds to the breakdown of smooth solutions of the inviscid Burgers-Hilbert equation (1.1). There is excellent numerical agreement between solutions of the asymptotic equation and small-amplitude solutions of the Burgers-Hilbert equation. Moreover, the singularity formation time of the asymptotic equation gives an accurate approximation of the singularity formation time of the Burgers-Hilbert equation for small initial data.

It follows that small, smooth solutions of the inviscid Burgers-Hilbert equation have a longer, cubically nonlinear lifespan than the quadratically nonlinear

lifespan of smooth solutions of the inviscid Burgers equation. This phenomenon is illustrated in Figure 8.4. The extension in the lifespan of smooth solutions is a result of the quadratic Burgers nonlinearity averaging out over a period of the temporal oscillations induced by the Hilbert transform. If part of the wave is compressed during one phase of the oscillation, then it is rarefied during the other phase. Thus, the nonlinear steepening of the wave profile in one phase is canceled by its expansion in the other.

The only explicit solution of (1.5) that we know of is the harmonic, spatially-periodic traveling-wave

$$(1.8) \quad \psi(x, t) = Ae^{ikx - i\omega t} \quad A \in \mathbb{C}, k > 0,$$

where ω satisfies the nonlinear dispersion relation

$$(1.9) \quad \omega = |A|^2 k^2.$$

We show that this solution is linearly and modulationally stable.

We conclude the introduction by outlining the contents of the paper. In Section 2, we discuss constant-frequency waves in the context of the general theory of nonlinear waves. In Section 3, we carry out a dimensional analysis of Hamiltonian wave motions which shows that the Burgers-Hilbert equation (1.1) is an appropriate model equation for unidirectional, constant-frequency surface waves. In Section 4, we use the method of multiple scales to derive the asymptotic equation (1.5) from (1.1). We outline the derivation of (1.5) for surface waves on a vorticity discontinuity in Appendix B. In Section 5, we describe the Hamiltonian structure of (1.5) and write the equation in equivalent spectral and real forms. In Section 6, we derive (1.5) from (1.1) by the use of a near-identity transformation. In Section 7, we show that harmonic solutions are linearly stable and derive a semi-classical approximation of (1.5). Finally, in Section 8, we present and compare some numerical solutions of (1.1) and (1.5).

2 Constant-frequency waves

We begin by recalling some well-known facts about dispersive and nondispersive hyperbolic waves [12, 13]. For simplicity, we consider a unidirectional, real-valued, wave motion with a single mode that propagates freely in space. Abusing notation, we write the linearized dispersion relation between the frequency ω and the wavenumber k of a harmonic wave as $\omega = \omega(k)$, where $\omega : \mathbb{R} \rightarrow \mathbb{R}$ is an odd function.

The wave motion is dispersive if $\omega'' \neq 0$, where the prime denotes a derivative with respect to k . According to the linearized theory, a small-amplitude dispersive wave spreads out into a locally harmonic wave-train. Over longer times, weakly nonlinear effects come into play, and the complex amplitude of the wave typically satisfies a cubically nonlinear Schrödinger equation.

Nondispersive hyperbolic waves have a dispersion relation of the form $\omega = c_0 k$, where c_0 is a constant wave-speed. According to the linearized theory, a wave

has an arbitrary spatial wave-profile that propagates at constant velocity without distortion. Over longer times, weakly nonlinear effects distort the wave-profile, and the profile of a bulk wave typically satisfies the quadratically nonlinear inviscid Burgers equation [2, 7].

The degree of nonlinearity in a weakly nonlinear equation is a consequence of the resonances allowed by the linearized dispersion relation. The quadratically nonlinear effects on nondispersive hyperbolic waves arise from three-wave resonances among harmonics of the form

$$\omega_1 = \omega_2 + \omega_3, \quad k_1 = k_2 + k_3.$$

Since $\omega = c_0 k$ this resonance condition is satisfied for any k_j such that $k_1 = k_2 + k_3$. As a result, the quadratically nonlinear self-interaction of an initially harmonic wave with frequency and wavenumber (ω, k) generates higher harmonics $(n\omega, nk)$ for every integer n . We assume throughout this discussion that all relevant nonlinear interaction coefficients are nonzero.

By contrast, three-wave resonances of dispersive waves do not occur (except in non-generic cases, such as second-harmonic resonance, which we do not consider). However, four-wave resonances of the form

$$\omega = \omega + \omega - \omega, \quad k = k + k - k$$

always occur. These resonances, and nearby ones, lead to cubically nonlinear effects on harmonics in a narrow frequency and wavenumber band about (ω, k) , but they do not lead to the resonant generation of higher harmonics $(\omega(nk), nk)$ for $|n| \neq 1$.

Constant-frequency waves have a linearized dispersion relation of the form

$$(2.1) \quad \omega = \omega_0 \operatorname{sgn} k$$

where ω_0 is a nonzero constant. The dispersion relation $\omega = \omega_0 \operatorname{sgn} k + c_0 k$ can be reduced to (2.1) by means of a Galilean transformation. Constant-frequency waves are nondispersive, since $\omega'' = 0$ for $k \neq 0$. According to the linearized theory, a constant-frequency wave has an arbitrary spatial profile that oscillates with frequency ω_0 between the profile and its Hilbert transform. Three-wave resonances do not occur since $\omega_0 \neq \omega_0 + \omega_0$, but four-wave resonances occur among any spatial harmonics with positive wavenumbers $\{k_1, k_2, k_3, k_4\}$ such that

$$(2.2) \quad k_1 = k_2 + k_3 - k_4, \quad k_j > 0.$$

The corresponding condition for the frequencies is satisfied automatically. Thus, cubically nonlinear interactions among different spatial harmonics generate new spatial harmonics, leading to a wide wavenumber spectrum but a narrow frequency spectrum. For example, in the case of spatially periodic waves with zero mean, we get a spectrum that consists of frequency and wavenumbers (ω_0, nk) for all nonzero integers n . The complex wave-amplitude function that describes the spatial profile of the wave typically satisfies a cubically nonlinear asymptotic equation, such as

(1.5). The nonlinear dynamics of constant-frequency waves is therefore fundamentally different from that of either dispersive waves or nondispersive hyperbolic waves.

3 Dimensional analysis

Constant-frequency waves arise in systems that are invariant under spatial scalings $(x, t) \mapsto (\lambda x, t)$. This invariance implies that the only space-time parameters on which the wave motion depends have the dimension of time; the motion cannot depend, for example, on parameters with the dimension of length, velocity, or acceleration. By contrast, nondispersive hyperbolic waves arise in systems that are invariant under space-time scalings $(x, t) \mapsto (\lambda x, \lambda t)$, which implies that the only space-time parameters on which the wave motion depends have the dimension of velocity.

In this section, we carry out a dimensional analysis of general Hamiltonian constant-frequency waves that explains why (1.1) provides an appropriate model equation for surface waves, such as waves on a vorticity discontinuity. A similar dimensional analysis [2] shows that the inviscid Burgers is an appropriate model equation for nondispersive hyperbolic bulk waves, such as nonlinear sound waves.

We consider a translation-invariant Hamiltonian wave motion [13] that depends upon two dimensional parameters: a frequency ω_0 and a density ρ_0 . We use M , L , T to denote the dimensions of mass, length, time, respectively, and denote the dimensions of a quantity X by $[X]$. Then $[\omega_0] = 1/T$ and $[\rho_0] = M/L^n$, where n is the number of space dimensions.

We denote canonically-conjugate complex wave amplitudes by $\{a(k), a^*(k)\}$ and suppose that they are parametrized by a wavenumber vector $k \in \mathbb{R}^d$. Thus, $d = n$ for bulk waves and $d = n - 1$ for waves that propagate along a surface of codimension one. The energy of the wave motion is given by a real-valued Hamiltonian functional $\mathcal{H}(a, a^*)$ of the wave amplitudes.

Assuming that the Hamiltonian is a smooth functional of the wave amplitudes, we Taylor expand it in powers of $\{a, a^*\}$ to get

$$\begin{aligned}
 \mathcal{H}(a, a^*) &= \int \omega_0 a(k) a^*(k) dk \\
 (3.1) \quad &+ \int \delta(k_1 - k_2 - k_3) V(k_1, k_2, k_3) a^*(k_1) a(k_2) a(k_3) dk_1 dk_2 dk_3 \\
 &+ \int \delta(k_1 + k_2 - k_3) V^*(k_1, k_2, k_3) a(k_1) a^*(k_2) a^*(k_3) dk_1 dk_2 dk_3 \\
 &+ O(|a|^4).
 \end{aligned}$$

Here, ω_0 is a constant frequency, and $V(k_1, k_2, k_3) \in \mathbb{C}$ is an interaction coefficient for the interaction $k_1 = k_2 + k_3$, which satisfies $V(k_1, k_2, k_3) = V(k_1, k_3, k_2)$. For simplicity, we suppose that the expansion of the Hamiltonian does not contain creation and annihilation terms, proportional to $a^*(k_1) a^*(k_2) a^*(k_3)$ and $a(k_1) a(k_2) a(k_3)$,

respectively. These terms are non-resonant and can be removed by a near identity transformation to the orders we consider here.

Since the Hamiltonian is an energy, it had dimension $[\mathcal{H}] = ML^2/T^2$, which implies that

$$[a] = \left(\frac{M}{T}\right)^{1/2} L^{1+d/2}, \quad [V] = \left(\frac{M}{T}\right)^{1/2} L^{3(1+d/2)+n}.$$

It follows that

$$V(k_1, k_2, k_3) = (\rho_0 \omega_0)^{1/2} W(k_1, k_2, k_3),$$

where $[W] = L^v$ with

$$v = \frac{n-d+2}{2}.$$

In particular, we have $v = 1$ for bulk waves and $v = 3/2$ for surface waves. The inverse wavenumber provides the only lengthscale for a constant-frequency wave-motion, so W is a homogeneous function of degree $-v$, meaning that

$$W(\lambda k_1, \lambda k_2, \lambda k_3) = \lambda^{-v} W(k_1, k_2, k_3) \quad \text{for all } \lambda > 0.$$

Next, we specialize to unidirectional waves and consider some examples of bulk and surface wave equations that are consistent with this dimensional argument.

3.1 Unidirectional waves

A unidirectional wave with a single, real-valued mode may be described by complex-canonical variables parameterized by a positive wavenumber

$$\{a(k), a^*(k) : 0 < k < \infty\}.$$

We consider a cubic, constant-frequency Hamiltonian without creation or annihilation terms,

$$\begin{aligned} \mathcal{H}(a, a^*) &= \int_0^\infty \omega_0 a(\xi) a^*(\xi) d\xi \\ (3.2) \quad &+ \int_0^\infty \int_0^\infty V(\xi + \eta, \xi, \eta) a^*(\xi + \eta) a(\xi) a(\eta) d\xi d\eta \\ &+ \int_0^\infty \int_0^\infty V^*(\xi + \eta, \xi, \eta) a(\xi + \eta) a^*(\xi) a^*(\eta) d\xi d\eta, \end{aligned}$$

where the interaction coefficient $V(k_1, k_2, k_3)$ is defined on positive wavenumbers k_j such that $k_1 = k_2 + k_3$ and is symmetric in (k_2, k_3) . The complex canonical form of Hamilton's equation is

$$(3.3) \quad ia_t(k, t) = \frac{\delta \mathcal{H}}{\delta a^*(k, t)} \quad \text{for } k > 0.$$

Using (3.2) in (3.3), we get the following equation for $a(k, t)$,

$$\begin{aligned} ia_t(k, t) &= \omega_0 a(k, t) + \int_0^k V(k, k - \xi, \xi) a(k - \xi, t) a(\xi, t) d\xi \\ &\quad + 2 \int_0^\infty V^*(k + \xi, k, \xi) a(k + \xi, t) a^*(\xi, t) d\xi \quad \text{for } k > 0. \end{aligned}$$

Defining $a(-k, t) = a^*(k, t)$, we may write this equation in convolution form as

$$\begin{aligned} i(\operatorname{sgn} k) a_t(k, t) &= \omega_0 a(k, t) \\ &\quad + \int_{-\infty}^\infty V(k, k - \xi, \xi) a(k - \xi, t) a(\xi, t) d\xi \quad \text{for } -\infty < k < \infty, \end{aligned}$$

where we extend $V(k_1, k_2, k_3)$ to a complex-valued function defined for all $k_j \in \mathbb{R}$ such that $k_1 = k_2 + k_3$. As shown in [2], this function is symmetric in $(-k_1, k_2, k_3)$ and satisfies $V(-k_1, -k_2, -k_3) = V^*(k_1, k_2, k_3)$.

The three-wave interaction coefficient of a constant-frequency bulk wave is a symmetric, homogeneous function of degree 1. A simple choice for it is

$$V(k_1, k_2, k_3) = (\rho_0 \omega_0)^{1/2} |k_1 k_2 k_3|^{1/3}$$

The corresponding Hamiltonian equation is

$$\begin{aligned} i(\operatorname{sgn} k) a_t(k, t) &= \omega_0 a(k, t) \\ &\quad + (\rho_0 \omega_0)^{1/2} |k|^{1/3} \int_{-\infty}^\infty |k - \xi|^{1/3} |\xi|^{1/3} a(k - \xi, t) a(\xi, t) d\xi. \end{aligned}$$

Introducing a non-canonical variable

$$u(x, t) = (\rho_0 \omega_0)^{1/2} \int_{-\infty}^\infty |k|^{1/3} a(k, t) e^{ikx} dk,$$

we get

$$u_t + \frac{1}{2} \mathbf{H} |\partial_x|^2 (u^2) = \omega_0 \mathbf{H} [u].$$

This equation, with a nonlocal nonlinearity, therefore provides a model Hamiltonian equation for constant-frequency bulk waves.

The three-wave interaction coefficient of a constant-frequency surface wave is a symmetric, homogeneous function of degree 3/2. A simple choice for it is

$$V(k_1, k_2, k_3) = (\rho_0 \omega_0)^{1/2} |k_1 k_2 k_3|^{1/2}.$$

The corresponding Hamiltonian equation is

$$\begin{aligned} i(\operatorname{sgn} k) a_t(k, t) &= \omega_0 a(k, t) \\ &\quad + (\rho_0 \omega_0)^{1/2} |k|^{1/2} \int_{-\infty}^\infty |k - \xi|^{1/2} |\xi|^{1/2} a(k - \xi, t) a(\xi, t) d\xi. \end{aligned}$$

Introducing the non-canonical variable

$$u(x, t) = (\rho_0 \omega_0)^{1/2} \int_{-\infty}^\infty |k|^{1/2} a(k, t) e^{ikx} dk,$$

we get the Burgers-Hilbert equation,

$$(3.4) \quad u_t + \left(\frac{1}{2} u^2 \right)_x = \omega_0 \mathbf{H}[u].$$

We may normalize $\omega_0 = 1$ in (3.4) by the scaling $t \mapsto \omega_0 t$, $u \mapsto \omega_0^{-1} u$, and the Hamiltonian form of the resulting equation is given in (1.2).

We remark that a simultaneous time-reversal and space-reflection leaves the linearized dispersion relation (2.1) invariant, but a separate time-reversal or space-reflection transforms $\omega_0 \mapsto -\omega_0$. Similarly, the transformation $t \mapsto -t$, $x \mapsto -x$, $u \mapsto u$ leaves (3.4) invariant, but a separate time-reversal $t \mapsto -t$, $u \mapsto -u$ or space-reflection $x \mapsto -x$, $u \mapsto -u$ transforms $\omega_0 \mapsto -\omega_0$. Thus, by making a spatial reflection if necessary, we can ensure that ω_0 is positive. It also follows that if a system is invariant under both time-reversal and space-reflection, then constant frequency modes must come in pairs, with the linearized dispersion relation $\omega^2 = \omega_0^2$.

For nondispersive hyperbolic waves depending on a wave speed c_0 , dimensional analysis [2] shows that the bulk-wave interaction coefficients are homogeneous of degree $3/2$, leading to an inviscid Burgers equation

$$u_t + c_0 u_x + \left(\frac{1}{2} u^2 \right)_x = 0.$$

This analysis explains why the local inviscid Burgers nonlinearity is appropriate for surface waves depending on a frequency ω_0 , and bulk waves depending on a speed c_0 .

4 The Burgers-Hilbert equation

In this section, we use the method of multiple scales to show that weakly nonlinear solutions of (1.1) satisfy the asymptotic equation (1.5). Before doing so, we shall briefly compare (1.1) with some other nonlinear, nonlocal wave equations that have been studied previously.

The Benjamin-Ono equation,

$$u_t + \left(\frac{1}{2} u^2 \right)_x + \mathbf{H}[u]_{xx} = 0,$$

contains a nonlocal, linear dispersive term but, unlike the term in (1.1), it is higher-order and prevents the formation of shocks. The inviscid Burgers equation with a lower-order source term consisting of a spatial convolution with an odd, integrable function $f: \mathbb{R} \rightarrow \mathbb{R}$,

$$(4.1) \quad u_t + \left(\frac{1}{2} u^2 \right)_x = f * u,$$

provides a useful model for nonlinear waves with a dispersion relation of the form $\omega = i\hat{f}(k)$ (see §13.14 of [12], §3.4.1 of [7], and [8], for example). One difference

between (4.1) and (1.1) is that convolution with an integrable function is a bounded linear operator on L^1 , whereas the Hilbert transform is a singular integral operator that is unbounded on L^1 . A more significant difference for the problems considered here is that (4.1) is dispersive, whereas (1.1) is nondispersive. As a result, small-amplitude solutions of (1.1) and (4.1) have qualitatively different behaviors.

The nonlinear, nonlocal equation

$$u_t = u\mathbf{H}[u],$$

introduced in [4] as a one-dimensional model for vortex stretching, includes a Hilbert transform in the nonlinearity, as does the equation

$$u_t = \left(\frac{1}{2}u^2\right)_{xx} + \mathbf{H}[u\mathbf{H}[u]_{xx}]$$

introduced in [6] as a model for nonlinear Rayleigh waves and derived in [1] for surface waves on a tangential discontinuity in magnetohydrodynamics.

4.1 Linearized equation

The linearization of (1.1) is

$$(4.2) \quad u_t = \mathbf{H}[u].$$

For definiteness, we consider solutions $u : \mathbb{R} \times \mathbb{R} \rightarrow \mathbb{R}$; with appropriate modifications, similar results apply to spatially periodic solutions $u : \mathbb{T} \times \mathbb{R} \rightarrow \mathbb{R}$.

The dispersion relation of (4.2) is $\omega = \text{sgn}k$, and the general solution is

$$u(x, t) = \int_0^\infty \left[\hat{\psi}(k)e^{ikx-it} + \hat{\psi}^*(k)e^{-ikx+it} \right] dk,$$

where $\hat{\psi} : (0, \infty) \rightarrow \mathbb{C}$ is arbitrary. Equivalently, we have

$$u(x, t) = \psi(x)e^{it} + \psi^*(x)e^{-it}$$

where $\psi : \mathbb{R} \rightarrow \mathbb{C}$ is given by

$$\psi(x) = \int_0^\infty \hat{\psi}(k)e^{ikx} dk.$$

It follows that $\mathbf{P}\psi = \psi$, where \mathbf{P} is the projection onto positive wavenumbers defined in (1.4). Writing

$$\psi(x) = \frac{f(x) + ig(x)}{2}$$

where f, g are real-valued functions, we find that $g = \mathbf{H}[f]$, and

$$u(x, t) = f(x) \cos t + \mathbf{H}[f](x) \sin t.$$

Thus, the spatial profile of the solution of (4.2) oscillates in time between f and $\mathbf{H}[f]$, where f is an arbitrary function.

Another way to understand this solution is to write $v = \mathbf{H}[u]$ and take the Hilbert transform of (4.2). Using the fact that $\mathbf{H}^2 = -\mathbf{I}$, we find that

$$u_t = v, \quad v_t = -u.$$

Thus, the linearized wave-motion consists of simple harmonic oscillators at each point of space. Oscillations at different points are coupled together only because their velocity is the spatial Hilbert transform of their displacement. Although the phase velocity $\omega/k = 1/|k|$ of the waves is nonzero, the group velocity ω' is zero, so the waves do not transport energy.

4.2 Weakly nonlinear waves

Next, we consider weakly nonlinear solutions of (1.1). Using the method of multiple scales, we look for an asymptotic solution of the form

$$(4.3) \quad u(x, t; \varepsilon) = \varepsilon u_1(x, t, \varepsilon^2 t) + \varepsilon^2 u_2(x, t, \varepsilon^2 t) + \varepsilon^3 u_3(x, t, \varepsilon^2 t) + O(\varepsilon^4).$$

We use (4.3) in (1.1), expand the result in power series with respect to ε , and equate coefficients of ε , ε^2 , ε^3 . We find that $u_1(x, t, \tau)$, $u_2(x, t, \tau)$, $u_3(x, t, \tau)$ satisfy

$$(4.4) \quad u_{1t} = \mathbf{H}[u_1],$$

$$(4.5) \quad u_{2t} + \left(\frac{1}{2}u_1^2\right)_x = \mathbf{H}[u_2],$$

$$(4.6) \quad u_{3t} + u_{1\tau} + (u_1 u_2)_x = \mathbf{H}[u_3].$$

The solution of (4.4) for u_1 is

$$(4.7) \quad u_1(x, t, \tau) = F(x, \tau)e^{-it} + F^*(x, \tau)e^{it},$$

where $F(\cdot, \tau) : \mathbb{R} \rightarrow \mathbb{C}$ satisfies

$$(4.8) \quad \mathbf{P}[F] = F.$$

We use (4.7) in (4.5) and solve the resulting equation for u_2 , to get

$$(4.9) \quad u_2(x, t, \tau) = G(x, \tau)e^{-2it} + M(x, \tau) + G^*(x, \tau)e^{2it},$$

$$(4.10) \quad G = -\left(\frac{1}{2}iF^2\right)_x, \quad M = -\mathbf{H}[FF^*]_x.$$

In solving for G , we use (4.8), which implies that $\mathbf{P}[F^2] = F^2$ and $\mathbf{H}[F^2] = -iF^2$.

We obtain an equation for F from the requirement that (4.6) is solvable for u_3 . To state this requirement, consider the following equation for $u(x, t)$,

$$(4.11) \quad u_t = \mathbf{H}[u] + B(x)e^{-int},$$

where $n \in \mathbb{Z}$ and $B : \mathbb{R} \rightarrow \mathbb{C}$.

Proposition 4.1. *If $n^2 \neq 1$, then (4.11) is uniquely solvable for every $B \in L^2(\mathbb{R})$. If $n = 1$, then (4.11) is solvable for $B \in L^2(\mathbb{R})$ if and only if*

$$(4.12) \quad \mathbf{P}[B] = 0,$$

and if $n = -1$, then (4.11) is solvable if and only if

$$(4.13) \quad \mathbf{Q}[B] = 0,$$

where \mathbf{P} and \mathbf{Q} are defined in (A.4).

Proof. A solution of (4.11) has the form

$$u(x, t) = A(x)e^{-int}$$

where A satisfies

$$(4.14) \quad inA + \mathbf{H}[A] = -B.$$

Taking the Hilbert transform of this equation, and using the fact that $\mathbf{H}^2 = -\mathbf{I}$, we get

$$(4.15) \quad A - in\mathbf{H}[A] = \mathbf{H}[B].$$

If $n^2 \neq 1$, the unique solution of (4.14)–(4.15) is

$$A = \frac{inB - \mathbf{H}[B]}{n^2 - 1}.$$

If $n = 1$, the system (4.14)–(4.15) is solvable if and only if $\mathbf{H}[B] = iB$. From (1.4), this means that B satisfies (4.12). In that case, the solution is

$$A = \frac{1}{2}iB + C$$

where $C(x)$ is an arbitrary function such that $\mathbf{P}[C] = C$. The solution for $n = -1$ is similar. \square

We use (4.7)–(4.10) in (4.6), compute the coefficient of the nonhomogeneous term proportional to e^{-it} , and impose the solvability condition (4.12) that its projection is zero. The solvability condition (4.13) follows by complex conjugation. After simplifying the result, we find that (4.6) is solvable for u_3 if and only if $F(x, \tau)$ satisfies

$$(4.16) \quad F_\tau = \mathbf{P} \left[F\mathbf{H}[FF^*]_x + iFF^*F_x \right]_x.$$

Equation (4.16) with $F = \psi$ and $\tau = t$ is equivalent to (1.5).

5 Properties of the asymptotic equation

In this section, we describe the formal Hamiltonian structure of the asymptotic equation (1.5), list the symmetries that we know of, and write it in equivalent spectral and real forms.

We denote by $\psi, \psi^* : \mathbb{R} \rightarrow \mathbb{C}$ complex-conjugate functions that satisfy the constraints

$$(5.1) \quad \mathbf{P}[\psi] = \psi, \quad \mathbf{Q}[\psi^*] = \psi^*,$$

where \mathbf{P} and \mathbf{Q} are the projections onto positive and negative wavenumber components, respectively, defined in (A.4). The functional derivative of a functional $\mathcal{H}(\psi, \psi^*)$ with respect to ψ^* is given by

$$\frac{\delta \mathcal{H}}{\delta \psi^*} = \mathbf{P}[h],$$

where $h : \mathbb{R} \rightarrow \mathbb{C}$ is any function such that

$$\left. \frac{d}{d\varepsilon} \mathcal{H}(\psi, \psi^* + \varepsilon \phi^*) \right|_{\varepsilon=0} = \int h \phi^* dx$$

for all $\phi^* : \mathbb{R} \rightarrow \mathbb{C}$ with $\mathbf{Q}[\phi^*] = \phi^*$. One may verify the Hamiltonian form of (1.5) directly by computing the functional derivative of \mathcal{H} given in (1.7) and using the result in (1.6).

5.1 Symmetries

The Hamiltonian (1.7) has the following symmetries.

- (1) Time translation invariance, $\psi(x, t) \mapsto \psi(x, t + \varepsilon)$, generated by the Hamiltonian \mathcal{H} .
- (2) Space translation invariance, $\psi(x, t) \mapsto \psi(x - \varepsilon, t)$, generated by the momentum

$$\mathcal{P} = \int \psi^* \psi dx.$$

- (3) Phase translation invariance, $\psi(x, t) \mapsto e^{-i\varepsilon} \psi(x, t)$, generated by the action

$$\mathcal{S} = \int \psi^* |\partial_x|^{-1} \psi dx.$$

- (4) Amplitude translation invariance, $\psi(x, t) \mapsto \psi(x, t) + \psi_0$ for any $\psi_0 \in \mathbb{C}$, generated for functions defined for $x \in \mathbb{R}$ by $-\psi_0 \mathcal{M}^*$, where

$$\mathcal{M} = \int x \psi dx.$$

The first three symmetries have a clear physical origin. The origin of the fourth symmetry is more mysterious. Its existence depends on a cancellation between the terms $in(\psi \psi_x^* - \psi^* \psi_x)$ and $n |\partial_x| n$ in the Hamiltonian (1.7), and it would not hold if the coefficients of those terms were in a different ratio.

The generating functionals of these symmetries are conserved quantities for (1.5). In addition, the Poisson bracket associated with $-\partial_x$,

$$(5.2) \quad \{\mathcal{F}, \mathcal{G}\} = - \int \frac{\delta \mathcal{F}}{\delta u} \partial_x \left[\frac{\delta \mathcal{G}}{\delta u} \right] dx,$$

has the Casimir functional

$$\mathcal{C} = \int \psi dx.$$

Thus if $x \in \mathbb{R}$, the functionals \mathcal{H} , \mathcal{P} , \mathcal{S} , \mathcal{M} , \mathcal{C} are conserved for smooth solutions of (1.5) that decay sufficiently rapidly at infinity (as may be verified directly from the equation). If $x \in \mathbb{T}$, the functionals \mathcal{H} , \mathcal{P} , \mathcal{S} , \mathcal{C} are conserved. We do not know, however, of an analog of \mathcal{M} for spatially periodic solutions.

5.2 Spectral form

Let $\hat{\psi}(k, t)$ denote the spatial Fourier transform of $\psi(x, t)$. The projection condition (1.4) implies that $\hat{\psi}(k, t) = 0$ for $k \leq 0$, so

$$\psi(x, t) = \int_0^\infty \hat{\psi}(k, t) e^{ikx} dx, \quad \psi^*(x, t) = \int_0^\infty \hat{\psi}^*(k, t) e^{-ikx} dx.$$

Using these expressions in the spatial expression of the Hamiltonian (1.7) and simplifying the result, we find that the spectral expression of the Hamiltonian is

$$(5.3) \quad \mathcal{H}(\hat{\psi}, \hat{\psi}^*) = \pi \int \delta(k_1 + k_2 - k_3 - k_4) \Lambda(k_1, k_2, k_3, k_4) \hat{\psi}(k_1) \hat{\psi}(k_2) \hat{\psi}^*(k_3) \hat{\psi}^*(k_4) dk_1 dk_2 dk_3 dk_4,$$

where δ denotes the delta-function, the integrals are taken over $k_j > 0$, and

$$(5.4) \quad \Lambda(k_1, k_2, k_3, k_4) = 2 \min\{k_1, k_2, k_3, k_4\}.$$

Writing (1.6) in terms of $\hat{\psi}$, we get

$$(5.5) \quad \hat{\psi}_t = -\frac{ik}{2\pi} \frac{\delta \mathcal{H}}{\delta \hat{\psi}^*}.$$

Use of (5.3) in (5.5) gives the spectral form of (1.5) for $\hat{\psi}(k, t)$

$$(5.6) \quad \hat{\psi}_t(k, t) + ik \int \delta(k + k_2 - k_3 - k_4) \Lambda(k, k_2, k_3, k_4) \hat{\psi}^*(k_2, t) \hat{\psi}(k_3, t) \hat{\psi}(k_4, t) dk_2 dk_3 dk_4 = 0 \quad \text{for } k > 0,$$

where Λ is defined in (5.4). This equation describes the evolution of a nonlinear wave due to four-wave resonant interactions (2.2) with the interaction coefficient Λ . One can also verify the result directly by taking the Fourier transform of (1.5).

5.3 Real form

To write the complex equation (1.5) for ψ in an equivalent real form, we define

$$(5.7) \quad v(x, t) = \psi(x, t) e^{-it} + \psi^*(x, t) e^{it}.$$

It follows that ψ is given in terms of v by

$$(5.8) \quad \psi(x, t) = \frac{1}{2} \{v(x, t) + i\mathbf{H}[v](x, t)\} e^{it}$$

The function v corresponds to the leading-order approximation for u in the expansion (4.3) and to the leading order approximation for the displacement η of a vorticity discontinuity in (B.1).

We differentiate (5.7) with respect to t , then use (1.5) and (5.8) to express the result in terms of spatial derivatives of v . After some algebra, whose details we omit, we find that $v(x, t)$ satisfies the equation

$$(5.9) \quad v_t + \partial_x \left\{ \frac{1}{6} |\partial_x| [v^3] - \frac{1}{2} v |\partial_x| [v^2] + \frac{1}{2} v^2 |\partial_x| [v] \right\} = \mathbf{H}[v].$$

Equation (5.9) has the Hamiltonian form

$$(5.10) \quad \begin{aligned} v_t + \partial_x \left[\frac{\delta \mathcal{H}}{\delta v} \right] &= 0, \\ \mathcal{H}(v) &= \int \left\{ \frac{1}{2} v |\partial_x|^{-1} [v] + \frac{1}{6} v^3 |\partial_x| [v] - \frac{1}{8} v^2 |\partial_x| [v^2] \right\} dx. \end{aligned}$$

6 Near-identity transformation

In this section, we derive the real form (5.9) of the asymptotic equation from the Burgers-Hilbert equation (1.1) by a symplectic near-identity transformation that removes the quadratically nonlinear terms from (1.1), which are nonresonant, and gives the cubically nonlinear terms in (5.9).

We introduce an amplitude parameter ε , and write the Hamiltonian in (1.2) for the Burgers-Hilbert equation (1.5) as

$$\mathcal{H} = \mathcal{H}_2 + \varepsilon \mathcal{H}_3,$$

where \mathcal{H}_j is homogeneous of degree j in u . Explicitly,

$$(6.1) \quad \mathcal{H}_2(u) = \int \frac{1}{2} u |\partial_x|^{-1} [u] dx, \quad \mathcal{H}_3(u) = \int \frac{1}{6} u^3 dx.$$

We define a symplectic, near-identity transformation $v \mapsto u(\varepsilon)$ by

$$u_\varepsilon + \partial_x \left[\frac{\delta \mathcal{F}}{\delta u} \right] = 0, \quad u(0) = v,$$

where the generating functional \mathcal{F} has the form

$$\mathcal{F}(u) = \mathcal{F}_3(u) + \varepsilon \mathcal{F}_4(u),$$

with \mathcal{F}_j homogeneous of degree j in u . Then, since $\mathcal{H}_\varepsilon = \{\mathcal{H}, \mathcal{F}\}$, where $\{\cdot, \cdot\}$ denotes the Poisson bracket (5.2), a Taylor expansion with respect to ε gives

$$(6.2) \quad \begin{aligned} \mathcal{H}(u(\varepsilon)) &= \mathcal{H}_2(v) + \varepsilon \left(\mathcal{H}_3 + \{\mathcal{H}_2, \mathcal{F}_3\} \right)(v) \\ &+ \varepsilon^2 \left(\{\mathcal{H}_2, \mathcal{F}_4\} + \{\mathcal{H}_3, \mathcal{F}_3\} + \frac{1}{2} \{ \{ \mathcal{H}_2, \mathcal{F}_3 \}, \mathcal{F}_3 \} \right)(v) + O(\varepsilon^3). \end{aligned}$$

To eliminate the cubically nonlinear terms from $\mathcal{H}(u)$, we choose

$$\mathcal{F}_3(v) = -\frac{1}{6} \int \mathbf{H}[v]^3 dx.$$

Using (A.2) and the fact that the Hilbert transform is a skew-adjoint isometry on L^2 , we compute that

$$\{\mathcal{H}_2, \mathcal{F}_3\} = -\mathcal{H}_3.$$

Thus, the cubic terms in (6.2) cancel, and we find that

$$(6.3) \quad \mathcal{H}(u(\varepsilon)) = \mathcal{H}_2(v) + \varepsilon^2 \mathcal{H}_4(v) + O(\varepsilon^3),$$

$$(6.4) \quad \mathcal{H}_4(v) = \{\mathcal{H}_2, \mathcal{F}_4\}(v) + \widetilde{\mathcal{H}}_4(v),$$

$$(6.5) \quad \widetilde{\mathcal{H}}_4(v) = \frac{1}{12} \int \left\{ \frac{2}{3} v^3 |\partial_x| [v] - \left(\mathbf{H}[v]^2 + \frac{1}{2} v^2 \right) |\partial_x| [v^2] \right\} dx.$$

The choice of \mathcal{F}_4 in the near-identity transformation and the form of the fourth-degree terms in the Hamiltonian is not uniquely determined. We choose

$$(6.6) \quad \mathcal{F}_4(v) = \int \left\{ \frac{1}{6} v_x \mathbf{H}[v] \mathbf{H}[v^2] - \frac{1}{8} \mathbf{H}[v]^2 (v^2)_x \right\} dx,$$

which leads to the asymptotic Hamiltonian. Using (6.1), (6.6), and (A.2)–(A.3) we compute that

$$(6.7) \quad \{\mathcal{H}_2, \mathcal{F}_4\}(v) = \frac{1}{12} \int \left\{ \mathbf{H}[v]^2 |\partial_x| [v^2] - v^2 |\partial_x| [v^2] + \frac{4}{3} v^3 |\partial_x| [v] \right\} dx.$$

The use of (6.5) and (6.7) in (6.4) then gives, after some simplification, that

$$(6.8) \quad \mathcal{H}_4(v) = \int_{-\infty}^{\infty} \left\{ \frac{1}{6} v^3 |\partial_x| [v] - \frac{1}{8} v^2 |\partial_x| [v^2] \right\} dx.$$

Neglecting terms of higher order than the quartic terms, setting the amplitude parameter ε equal to one, and using (6.1), (6.8) in (6.3), we see that the near-identity transformation $v \mapsto u$ generated by \mathcal{F} , transforms the Hamiltonian equations (1.2) into (5.10).

Up to quadratic terms, generated by \mathcal{F}_3 , the near identity transformation is given by

$$u = v - \frac{1}{2} |\partial_x| (\mathbf{H}[v]^2) + \dots$$

One may verify directly using (A.2) that this transformation eliminates the quadratically nonlinear terms from (1.1).

7 Stability of periodic waves

The harmonic-wave solution (1.8)–(1.9) is a constant-frequency analog of the Stokes-wave solution for the NLS equation. A significant difference, however, is that the dependence of the frequency on the wave amplitude A is multiplicative, rather than additive.

A single positive-wavenumber harmonic is an exact solution of (1.5) because four-wave resonant interactions of the form $k + k - k$ do not generate any new spatial harmonics. On the other hand, resonant interactions that involve more than one spatial harmonic generate infinitely many new harmonics (for example, $3k = 2k + 2k - k$, $4k = 3k + 2k - k$, and so on).

7.1 Linearized stability

To study the linearized stability of the solution (1.8)–(1.9), we normalize $A = k = \omega = 1$, without loss of generality, and write

$$(7.1) \quad \psi(x, t) = e^{i(x-t)} [1 + \phi(x, t)].$$

Using this expression in (1.5), and linearizing the result with respect to ϕ , we get

$$\phi_t - i\phi = e^{-ix} \mathbf{P} \left[e^{ix} \left(|\partial_x| [m] - m + i\phi_x - \phi \right) \right]_x$$

where $m = \phi + \phi^*$. We write this equation as

$$\phi_t - i\phi = \tilde{\partial}_x \tilde{\mathbf{P}} \left[|\partial_x| [\phi^*] - \phi^* + |\partial_x| [\phi] + i\phi_x - 2\phi \right]$$

where

$$\tilde{\partial}_x = e^{-ix} \partial_x e^{ix} = \partial_x + i\mathbf{I}, \quad \tilde{\mathbf{P}} = e^{-ix} \mathbf{P} e^{ix}.$$

The Fourier transform $\hat{\psi}(k, t)$ is supported in $0 < k < \infty$, so from (7.1) $\hat{\phi}(k, t)$ is supported in $-1 < k < \infty$. It follows that $\tilde{\mathbf{P}}[\phi] = \phi$, and therefore

$$\phi_t - i\phi = \tilde{\partial}_x \tilde{\mathbf{P}} \left[|\partial_x| [\phi^*] - \phi^* \right] + (\partial_x + i) (|\partial_x| [\phi] + i\phi_x - 2\phi).$$

To compute the action of $\tilde{\mathbf{P}}$ on ϕ^* , we decompose ϕ as

$$\phi(x, t) = \xi(x, t) + \eta(x, t)$$

where

$$\xi(x, t) = \int_{-1}^1 \hat{\phi}(k, t) e^{ikx} dk, \quad \eta(x, t) = \int_1^{\infty} \hat{\phi}(k, t) e^{ikx} dk.$$

Then

$$\tilde{\partial}_x \tilde{\mathbf{P}} \left[|\partial_x| [\phi^*] - \phi^* \right] = (\partial_x + i\mathbf{I}) \left[|\partial_x| [\xi^*] - \xi^* \right],$$

and

$$(7.2) \quad \phi_t + 3\phi_x - i|\partial_x|[\phi] + i\phi = |\partial_x|[\phi]_x + i\phi_{xx} + (\partial_x + i) (|\partial_x|[\xi^*] - \xi^*).$$

Projecting (7.2) onto Fourier components with $1 < k < \infty$, and using the fact that $|\partial_x|[\eta] = -i\eta_x$, we get

$$\eta_t + 2\eta_x + i\eta = 0.$$

Thus, perturbations with wavenumber $k > 1$ are independent of the other modes. They are stable, with velocity 2 and frequency 1.

Projecting (7.2) onto Fourier components with $-1 < k < 1$, we get

$$(7.3) \quad \xi_t + 3\xi_x - i|\partial_x|[\xi] + i\xi = |\partial_x|[\xi]_x + i\xi_{xx} + (\partial_x + i) (|\partial_x|[\xi^*] - \xi^*).$$

Thus, if $0 < k < 1$, the k and $(-k)$ modes are coupled through their interaction with the unperturbed wave.

To solve (7.3), we write

$$\xi(x, t) = \mu(x, t) + \nu^*(x, t)$$

where

$$\mu(x, t) = \int_0^1 \hat{\phi}(k, t) e^{ikx} dk, \quad v(x, t) = \int_0^1 \hat{\phi}^*(-k) e^{ikx} dk.$$

Then $\mathbf{H}[\mu] = -i\mu$, $\mathbf{H}[v] = -iv$ and

$$|\partial_x|[\xi] = -i\mu_x + iv_x^*.$$

Using this equation in (7.3), projecting the result onto Fourier components with $0 < k < 1$ and $-1 < k < 0$, respectively, and simplifying the result, we get

$$\begin{aligned} \mu_t + 2\mu_x + i\mu + i(\partial_x^2 + 1)v &= 0, \\ v_t + 4v_x - iv + 2iv_{xx} + i(\partial_x - i)^2\mu &= 0. \end{aligned}$$

We look for Fourier solutions of this system of the form

$$\mu(x, t) = Me^{ikx - i\omega t}, \quad v(x) = Ne^{ikx - i\omega t}$$

where $0 < k < 1$. Then

$$\begin{bmatrix} -\omega + 2k + 1 & 1 - k^2 \\ -(1 - k)^2 & -\omega - 1 + 4k - 2k^2 \end{bmatrix} \begin{bmatrix} M \\ N \end{bmatrix} = 0.$$

Setting the determinant of the matrix in this equation equal to zero, and introducing the phase speed $c = \omega/k$, we get

$$c^2 + 2(k - 3)c + 6 - 2k - k^2 = 0.$$

The solutions are real, with

$$(7.4) \quad c = (3 - k) \pm \sqrt{1 + 2(1 - k)^2}.$$

It follows that the harmonic solutions (1.8)–(1.9) of (1.5) are linearly stable to small perturbations.

We remark that in this analysis, unlike the analogous analysis of dispersive waves using the NLS equation, the perturbations are not assumed to be of long wavelength relative to the wavelength of the carrier wave. Their frequency is, however, close to the frequency of the carrier wave.

7.2 Semi-classical approximation

To derive a semi-classical approximation for (1.5) it is convenient to proceed informally. We write

$$(7.5) \quad \psi(x, t) = a(x, t) e^{iS(x, t)}$$

where a, S are real-valued functions. Using (7.5) in (1.5), we get

$$(7.6) \quad iaS_t + a_t = e^{-iS} \mathbf{P} \left[\{ a |\partial_x| [a^2] - a^3 S_x + ia^2 a_x \} e^{iS} \right]_x.$$

We suppose that the phase S varies much more rapidly than a , so that the spectrum of ψ is concentrated near S_x . Assuming that $S_x > 0$, we have for any slowly varying function b that

$$\mathbf{P} [be^{iS}] \sim be^{iS}.$$

We may therefore approximate (7.6) by

$$iaS_t + a_t = iS_x \{a |\partial_x| [a^2] - a^3 S_x + ia^2 a_x\} \\ + \{a |\partial_x| [a^2] - a^3 S_x + ia^2 a_x\}_x.$$

Expanding derivatives and equating real and imaginary parts in this equation we get

$$S_t + a^2 S_x^2 = S_x |\partial_x| [a^2] + aa_{xx} + 2a_x^2, \\ a_t + 4S_x a^2 a_x + a^3 S_{xx} = (a |\partial_x| [a^2])_x.$$

Introducing $n = a^2$ and $k = S_x$, we may write these equations as

$$(7.7) \quad k_t + (k^2 n)_x = \left(k |\partial_x| [n] + \frac{1}{2} n_{xx} + \frac{n_x^2}{4n} \right)_x, \\ n_t + (2kn^2)_x = 2n |\partial_x| [n]_x + n_x |\partial_x| [n].$$

The terms on the right-hand side of (7.7) are small in the semi-classical limit. The leading order semi-classical equations are therefore

$$(7.8) \quad k_t + (k^2 n)_x = 0, \\ n_t + (2kn^2)_x = 0.$$

These equations form a hyperbolic system for (k, n) :

$$(7.9) \quad \begin{bmatrix} k \\ n \end{bmatrix}_t + \begin{bmatrix} 2kn & k^2 \\ 2n^2 & 4kn \end{bmatrix} \begin{bmatrix} k \\ n \end{bmatrix}_x = 0.$$

The eigenvalues λ and eigenvectors R of the matrix in (7.9) are given by

$$\lambda = \gamma kn, \quad R = \begin{bmatrix} k \\ (\gamma - 2)n \end{bmatrix}$$

where

$$(7.10) \quad \gamma = 3 \pm \sqrt{3}.$$

The hyperbolicity of the semi-classical equations means that periodic wavetrains are modulationally stable, and is consistent with the linearized stability of periodic waves. The characteristic velocities $\lambda = 3 \pm \sqrt{3}$ of (7.8) at $kn = 1$ agree with the velocities in $c = 3 \pm \sqrt{3}$ at $k = 0$ in (7.4), both of which limits describe linearized, long-wave perturbations of the solution $\psi(x, t) = e^{ix-it}$.

Riemann invariants Φ of (7.9) are given by

$$\Phi(k, n) = kn^{(\gamma-2)/2}.$$

It follows that $\{(k, n) : k > 0, n > 0\}$ is an invariant region for smooth solutions of (7.9), consistent with the assumption made in deriving the system that $k, n > 0$.

The characteristics of (7.9) are genuinely nonlinear for $kn \neq 0$, with

$$(7.11) \quad \nabla \lambda \cdot R = \beta kn, \quad \beta = 9 \pm 5\sqrt{3}.$$

Thus, in general, semi-classical solutions steepen until the higher-order dispersive terms on the right hand side of (7.7) become important.

The dominant long-wave dispersive terms in (7.7) are the ones proportional to $|\partial_x| [n]_x = \mathbf{H}[u]_{xx}$. Omitting the explicit introduction of a small parameter, we find that small-amplitude, long-wave perturbations of k , n about $k = 1$, $n = 1$ are given by

$$k(x, t) = 1 + u(x, t) + \dots, \quad n(x, t) = 1 + (\gamma - 2)u(x, t) + \dots,$$

where $u(x, t)$ satisfies a Benjamin-Ono equation

$$(7.12) \quad u_t + \gamma u_x + \beta u u_x = \alpha \mathbf{H}[u]_{xx}.$$

Here, γ is the linearized wave speed (7.10), β is the genuine-nonlinearity coefficient (7.11), and

$$\alpha = 1 \pm \frac{2\sqrt{3}}{3}$$

is a linear dispersive coefficient. This value agrees with the long-wave expansion of the linearized phase velocity (7.4), which is $c = \gamma - \alpha|k| + O(k^2)$ as $k \rightarrow 0$.

The soliton solutions of (7.12) are

$$u(x, t) = \frac{4\alpha}{\beta} \left[\frac{a}{(x - ct)^2 + a^2} \right]$$

where a is a large, positive parameter, and

$$c = \gamma + \frac{\alpha}{a}.$$

For the (+)-branch, with $\alpha > 0$, the solitons travel faster than periodic long waves, while for the (-)-branch, with $\alpha < 0$, the solitons travel slower than periodic long waves. The solitons have the same phase velocity as a periodic short wave with wavenumber close to $\kappa = 4 \pm 2\sqrt{3}$. This suggests that solitary waves corresponding to the BO-solitons may not exist in the full asymptotic equation due to the radiation of short waves, but we will not pursue that question further here.

8 Numerical solutions

We used a pseudo-spectral method to numerically integrate both the Burgers-Hilbert equation (1.1) and the asymptotic equation (1.5). We computed the spatial derivatives and the Hilbert transform spectrally, and carried out the time-integration by means of a fourth order Runge-Kutta scheme. The numerical solutions show that small-amplitude solutions of the Burgers-Hilbert equation are well-described by the corresponding solutions of the asymptotic equation. They also show that solutions of the asymptotic equation steepen and form a singularity.

Using 2^{12} points for $x \in [0, 2\pi]$, we could integrate the equations quickly in MATLAB up to the formation-time of the singularity, which will be discussed below. For both equations, energy was conserved to within a relative error of less than 10^{-7} for the duration of the integration; and, for the asymptotic equation, the momentum and action were conserved to within a relative error of less than 10^{-8} .

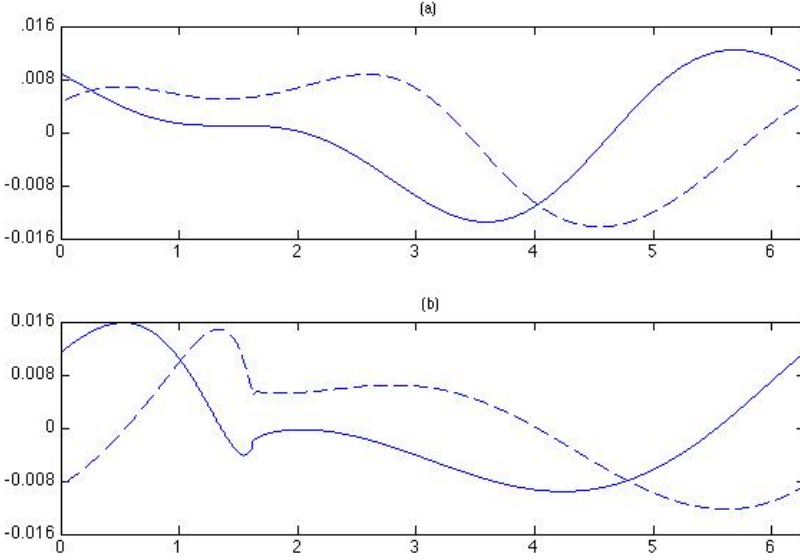


FIGURE 8.1. A numerical solution of the Burgers-Hilbert equation (1.1) for the initial condition (8.1) with $A = 0.01$. (a) The solid line shows $u(x, 0)$. The dashed line shows the solution $u(x, \pi/2)$, one quarter-period after the initial condition. (b) The solution for the initial condition in (a) just prior to the formation of a singularity. The solid and dashed line show $u(x, T_s)$ for $T_s = 2\pi n$ for $n = 10^4$ and $n = 10^4 + 1/4$, respectively.

We performed several integrations of the Burgers-Hilbert equation with the same initial profile scaled to different amplitudes:

$$(8.1) \quad u(x, 0) = A \left\{ \cos x + \frac{1}{2} \cos [2(x + 2\pi^2)] \right\}$$

where A is a real constant. This data has maximum negative slope

$$\varepsilon = |\min u_x(x, 0)|$$

where $\varepsilon = cA$ with $c \approx 1.225$.

A linear timescale T_h for (1.1) is given by the period $T_h = 2\pi$ of solutions of the linearized equation (4.2). A nonlinear timescale T_b is given by the shock formation time $T_b = 1/\varepsilon$ for the inviscid Burgers equation. Thus,

$$2\pi\varepsilon = \frac{T_h}{T_b}$$

is an appropriate parameter for measuring the effect of nonlinearity on solutions of the Burgers-Hilbert equation. If ε is small, which is the regime in which the

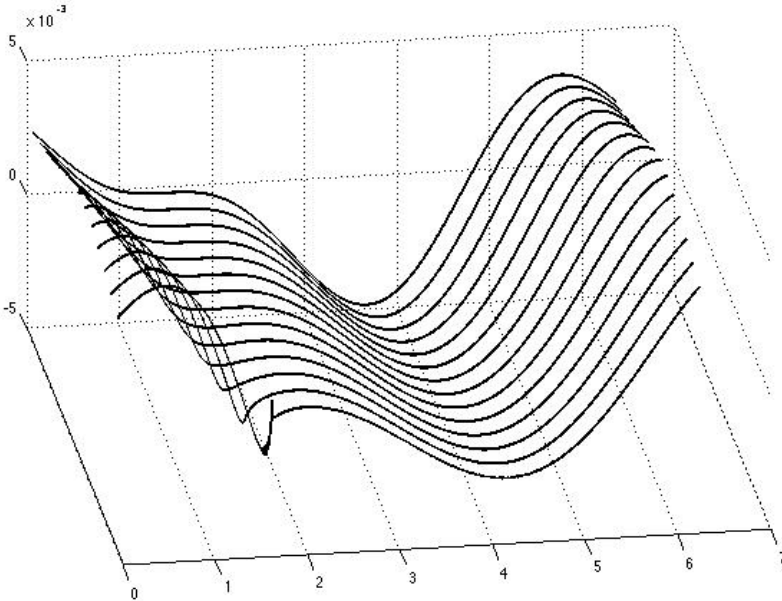


FIGURE 8.2. Snapshots of $u(x,t)$ for the solution in figure 8.1. Time increases to the foreground from the initial condition to the development of the singularity, and each time slice is taken at an integer multiple of 2π in order to factor out the fast oscillation. The singularity develops as a steepening ahead of the maximum of $-u_x(x,0)$.

asymptotic equation applies, then singularities form over the course of many oscillations; while if ε is large, they form quickly relative to the period of a single oscillation.

For smaller amplitude data, with $2\pi\varepsilon \leq 1.2$, the solutions evolve in a qualitatively similar fashion. Over shorter times, they approximately oscillate with period 2π between a profile and its Hilbert transform. Over longer times, the profile deforms and steepens until a singularity in the derivative u_x develops.

Figure 8.1 shows a numerical solution of (1.1) for the initial data (8.1) with $A = 10^{-2}$ and $\varepsilon \approx 1.2 \times 10^{-2}$. In the top frame of figure 8.1, the solid line is the initial data and the dashed line is the solution at $t = \pi/2$. The dashed line is almost equal to the Hilbert transform of the solid line. In the bottom frame of figure 8.1, the solid line shows the solution $u(x,t)$ at $t = 2\pi n$ with $n = 10^4$, just prior to the development of the singularity, and the dashed line shows the solution at $t = 2\pi n + \pi/2$. The dashed curve is again almost equal to the Hilbert transform of the solid curve.

Several snapshots in time of $u(x,t)$ are shown in figure 8.2 where the times of each slice are integer multiples of the linearized oscillation period. The singularity

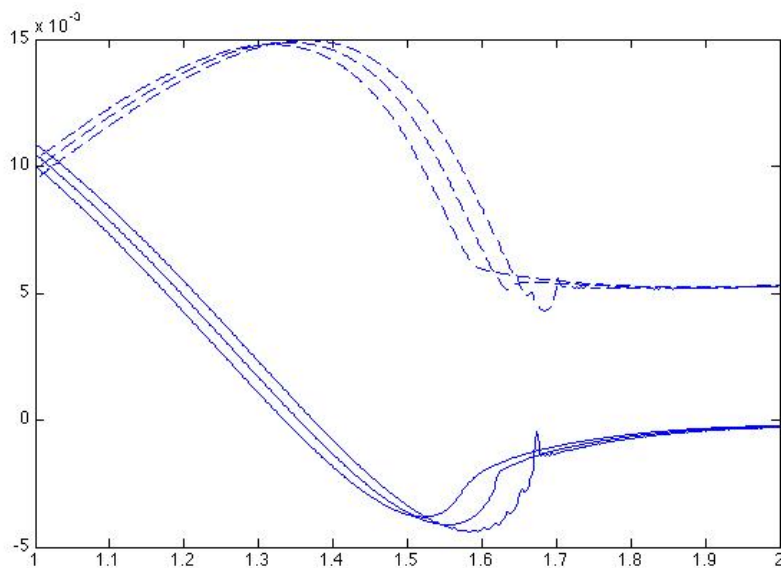


FIGURE 8.3. Magnification of $u(x,t)$ near the singularity for the solution in figure 8.1. The solid curves show the solution one period before, at, and one period after the time of singularity formation. The dashed curves show the solution a quarter period before, a quarter period after, and one and a quarter periods after the time of singularity formation; they are approximately the Hilbert transforms of the solid curves.

develops ahead of a peak in u . The solution steepens in a similar fashion to solutions of the Burgers equation, but the Burgers-Hilbert equation has an additional fast oscillation which has been factored out of the plot.

As the singularity forms, the solution of the Burgers-Hilbert equation develops a small-scale structure, which is shown in figure 8.3. We determined the time T_s and location of singularity-formation numerically. The solid lines show the solution near the location of the singularity at times $T_s - 2\pi$, T_s and $T_s + 2\pi$. The dashed lines show the solution at times $T_s - 1.5\pi$, $T_s + 0.5\pi$ and $T_s + 2.5\pi$. In both phases, the wave-profile forms a small dip ahead of its steepest part, followed by a corner, or 'knee', after which the profile becomes relatively flat. The integration can be continued to times slightly beyond the development of the singularity, presumably because de-aliasing in the pseudo-spectral method introduces a small amount of numerical dissipation and dispersion.

For larger amplitude data, with $2\pi\epsilon \geq 1.7$, the qualitative nature of the solution is dramatically different. The characteristic time of the nonlinear term, $T_b = 1/\epsilon < 3.7$, is then significantly less than the period 2π of the linear term. The solutions do not oscillate between one profile and its Hilbert transform; instead, they develop

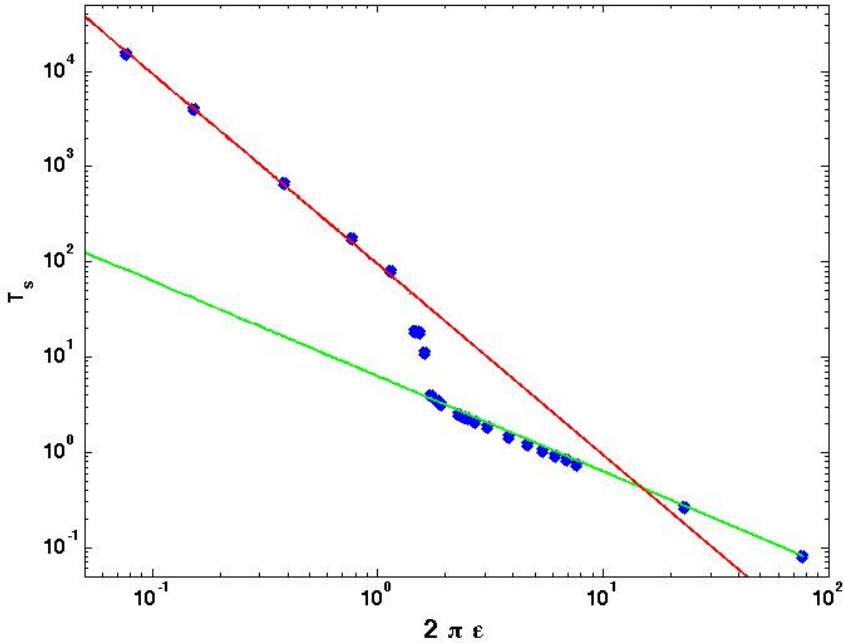


FIGURE 8.4. Logarithm of the singularity formation time T_s for the Burgers-Hilbert equation versus the logarithm of $2\pi\epsilon$ for the numerical experiments (diamonds) along with the prediction from the asymptotic equation, $T_s = 2.37 \epsilon^{-2}$ (steeper line) and the prediction from the Burgers equation $T_s = \epsilon^{-1}$ (shallower line).

shocks in similar way to solutions of the Burgers equation. In this regime, the asymptotic equation no longer provides a good approximation for the evolution of u .

The transition between these two qualitatively different regimes is remarkably rapid. For example, when $2\pi\epsilon = 1.154$, the singularity forms at time $T_s \approx 77.9$ in the twelfth oscillation of period 2π ; but when $2\pi\epsilon = 1.731$, the singularity forms at $T_s \approx 3.94$ in the first oscillation. Thus, once the data is small enough that a singularity does not form in the first few oscillations, the effect of the nonlinearity becomes much weaker as a result of the alternation between compression and expansion in each oscillation, leading to a greatly increased lifespan of smooth solutions.

Figure 8.4 shows a log-log plot of the numerically computed singularity-formation time T_s against $2\pi\epsilon$ for several integrations. The equation

$$(8.2) \quad \epsilon^2 T_s = 2.37$$

provides an excellent fit to the numerical values for $2\pi\epsilon \leq 1$. The scaling $T_s \sim k \epsilon^{-2}$ as $\epsilon \rightarrow 0$ agrees with the cubically-nonlinear scaling used to derive the asymptotic

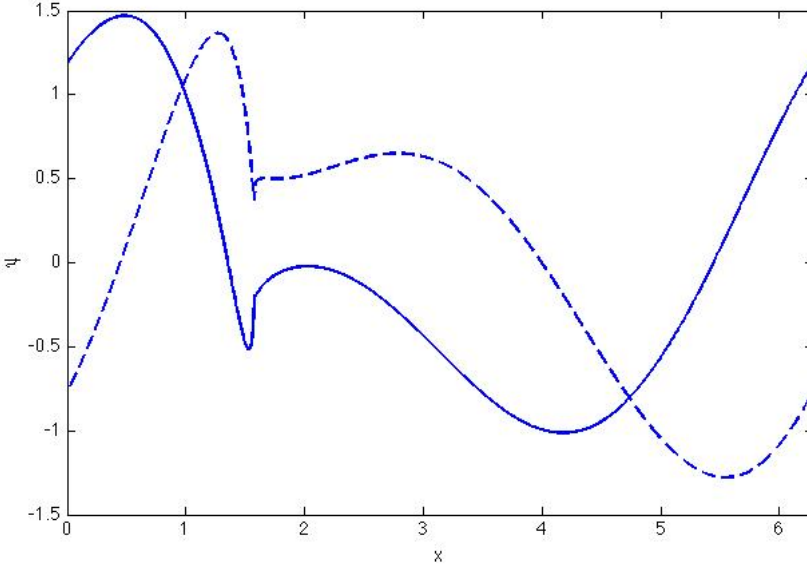


FIGURE 8.5. The solution of the asymptotic equation (1.5) with initial data (8.3) at the onset of the singularity. The solid line is $\Re(\psi)$, the dashed line is $\Im(\psi)$. Compare with figure 8.1 (b).

equation (1.5) from equation (1.1), and the value $k \approx 2.37$ is obtained from the numerical integration of the asymptotic equation described below.

For large values of ε , we expect that (1.1) should behave like the inviscid Burgers equation and that

$$T_s \sim \varepsilon^{-1} \quad \text{as } \varepsilon \rightarrow \infty.$$

This line is also plotted on figure 8.4; the agreement with the numerical values is excellent for $2\pi\varepsilon \geq 2$.

In the transition regime, $1.2 < 2\pi\varepsilon < 1.7$, the singularity-formation time T_s appears to increase in a series of steps as ε decreases. These results suggest that $T_s : (0, \infty) \rightarrow \mathbb{R}$ is a decreasing, lower-semicontinuous function of ε with jump discontinuities at a decreasing sequence $\{\varepsilon_n : n \in \mathbb{N}\}$ of values of ε , where ε_n is the largest value of ε for which the singularity forms in the n^{th} oscillation. We further expect that $\varepsilon_n \rightarrow 0$ as $n \rightarrow \infty$ and

$$T_s(\varepsilon_{n+1}) - T_s(\varepsilon_n) \sim 2\pi.$$

Next, we describe a numerical solution of the asymptotic equation. We integrated (1.5) for $\psi(x, t)$ with initial data

$$(8.3) \quad \psi(x, 0) = e^{ix} + \frac{1}{2}e^{2i(x+2\pi^2)}.$$

The corresponding asymptotic solution of the Burgers-Hilbert equation (1.1) with initial data (8.1) is

$$u(x, t) \sim \frac{1}{2}A \psi \left(x, \frac{1}{4}A^2t \right) e^{-it} + \text{c.c.} \quad \text{as } A \rightarrow 0.$$

The real and imaginary parts of $\psi(x, t)$ are shown in figure 8.5 just prior to the development of the singularity at $t = \tau_s$ where $\tau_s \approx 0.395$. Since u oscillates between the real and imaginary parts of ψ on the fast time scale, the curves in figure 8.5 should be compared to the corresponding curves in figure 8.1 (b). While $\Im(\psi)$ shows a sharper feature right at the point of the singularity, the two figures otherwise agree extremely well with each other.

The asymptotic theory predicts that the singularity formation time T_s for the Burgers-Hilbert equation has the asymptotic behavior

$$T_s \sim 4\tau_s A^{-2} \quad \text{as } A \rightarrow 0.$$

Setting $A = \varepsilon/c$, and using the numerically computed value for τ_s , we get

$$T_s \approx 2.37\varepsilon^{-2} \quad \text{as } \varepsilon \rightarrow 0.$$

which is the relation used to fit the Burgers-Hilbert data in equation (8.2). The mean of $\varepsilon^2 T_s$ for the five values of ε from the Burgers-Hilbert data whose T_s lie near the asymptotic fit is given by

$$\overline{\varepsilon^2 T_s} = 2.47.$$

This differs by 4% from the coefficient predicted by the asymptotic equation; moreover, the difference is less for the smaller values of ε . Thus, the solution of the asymptotic equation is in excellent quantitative agreement with the solutions of the Burgers-Hilbert equation.

Appendix A: Notation

In this appendix, we define and summarize notation that is used throughout the paper. For definiteness, we consider square-integrable functions defined on \mathbb{R} . Similar considerations apply to periodic functions, in which case we project constant Fourier modes to zero.

We denote the Fourier transform of $f \in L^2(\mathbb{R})$ by $\hat{f} \in L^2(\mathbb{R})$, where

$$f(x) = \int_{-\infty}^{\infty} \hat{f}(k) e^{ikx} dk.$$

The Hilbert transform $\mathbf{H} : L^2(\mathbb{R}) \rightarrow L^2(\mathbb{R})$ is defined by

$$\widehat{\mathbf{H}[f]}(k) = -i(\text{sgn } k)\hat{f}(k),$$

where

$$(A.1) \quad \text{sgn } k = \begin{cases} +1 & \text{if } k > 0, \\ 0 & \text{if } k = 0, \\ -1 & \text{if } k < 0, \end{cases}$$

Equivalently,

$$\mathbf{H}[f] = \left(\text{p.v.} \frac{1}{\pi x} \right) * f.$$

The Hilbert transform is a skew-adjoint isometry on $L^2(\mathbb{R})$, and $\mathbf{H}^2 = -\mathbf{I}$.

If $u : \mathbb{R} \rightarrow \mathbb{R}$ is a real-valued L^2 -function, then $u + i\mathbf{H}[u]$ is the boundary value on the real axis of a function that is holomorphic in the upper-half plane with uniformly bounded L^2 -norms on lines with constant positive imaginary part. If F and G are holomorphic functions whose boundary values have real parts v and w , respectively, then a consideration of the holomorphic functions FG and F^3 shows that, under suitable assumptions on v and w ,

$$(A.2) \quad \mathbf{H} \left[vw - \mathbf{H}[v]\mathbf{H}[w] \right] = v\mathbf{H}[w] + w\mathbf{H}[v],$$

$$(A.3) \quad v^2\mathbf{H}[v] - \frac{1}{3}\mathbf{H}[v]^3 = \mathbf{H} \left[\frac{1}{3}v^3 - v\mathbf{H}[v]^2 \right].$$

For example, it is sufficient that $v, w \in L^p$ for $p > 2$ in (A.2), and $v \in L^p$ for $p > 3$ in (A.3).

We define orthogonal self-adjoint projections

$$\mathbf{P}, \mathbf{Q} : L^2(\mathbb{R}) \rightarrow L^2(\mathbb{R})$$

onto positive and negative wavenumber components by

$$(A.4) \quad \mathbf{P} = \frac{1}{2}(\mathbf{I} + i\mathbf{H}), \quad \mathbf{Q} = \frac{1}{2}(\mathbf{I} - i\mathbf{H}).$$

Then

$$\mathbf{P}[f]^* = \mathbf{Q}[f^*], \quad \mathbf{Q}[f]^* = \mathbf{P}[f^*],$$

where the star denotes the complex conjugate, and

$$\int_{-\infty}^{\infty} \mathbf{P}[f](x)g(x)dx = \int_{-\infty}^{\infty} f(x)\mathbf{Q}[g](x)dx.$$

We denote the differentiation operator by ∂_x , and define

$$|\partial_x| = \mathbf{H}\partial_x, \quad \widehat{|\partial_x|[f]}(k) = |k|\hat{f}(k).$$

Appendix B: Surface waves on a vorticity discontinuity

In this appendix, we study surface waves on an interface between two half-spaces with constant vorticities in a two-dimensional, inviscid, incompressible fluid shear flow. We suppose that the unperturbed interface is located at $y = 0$, and denote the vorticities in $y > 0$ and $y < 0$ by $-\alpha_+$ and $-\alpha_-$, respectively, where $\alpha_+ \neq \alpha_-$. We denote the location of the perturbed interface by $y = \eta(x, t; \varepsilon)$.

First, we summarize the asymptotic solution. The location of the vorticity discontinuity is given by

$$(B.1) \quad \eta(x, t; \varepsilon) = \varepsilon \left\{ F(x, \varepsilon^2 t) e^{-i\alpha_0 t} + F^*(x, \varepsilon^2 t) e^{i\alpha_0 t} \right\} + O(\varepsilon^2) \quad \text{as } \varepsilon \rightarrow 0,$$

where $F(x, \tau)$ satisfies

$$(B.2) \quad F_\tau = \gamma_0 \mathbf{P} \partial_x \left[F |\partial_x| [FF^*] + iFF^*F_x \right], \quad \mathbf{P}[F] = F.$$

The frequency parameters ω_0 and γ_0 in (B.1)–(B.2) are given by

$$(B.3) \quad \omega_0 = \frac{\alpha_+ - \alpha_-}{2}, \quad \gamma_0 = \frac{\alpha_+^2 + \alpha_-^2}{\alpha_+ - \alpha_-}.$$

Equation (B.2) with $F = \psi$, and $\gamma_0 \tau = t$ is equivalent to (1.5).

After accounting for the coefficients, we find that (B.2) is identical to the asymptotic equation derived in Section 4 for the Burgers-Hilbert equation

$$(B.4) \quad \eta_t + \left(\frac{1}{2} \beta_0 \eta^2 \right)_x = \omega_0 \mathbf{H}[\eta], \quad \beta_0^2 = \frac{\alpha_+^2 + \alpha_-^2}{2}.$$

Either choice of sign for β_0 in (B.4) leads to the same asymptotic equation (B.2). This is because the transformation $\eta \mapsto -\eta$ corresponds to a half-period phase shift in the linearized oscillations and does not affect the averaged, long-time dynamics.

Since (B.4) leads to the same asymptotic equation as the one derived from the primitive fluid equations, it provides an effective equation for the motion of a planar vorticity discontinuity with slope of the order ε , over times of the order $\omega_0^{-1} \varepsilon^{-2}$. The coefficient β_0 in (B.4) is not equal to the coefficient α_0 of the quadratic nonlinearity in the equations of motion for a vorticity discontinuity, which, from (B.15) below, is given by

$$(B.5) \quad \alpha_0 = \frac{\alpha_+ + \alpha_-}{2}.$$

Instead, β_0 describes the combined effect of both quadratic and cubic nonlinearities. For example, if the shear flow is symmetric and $\alpha_+ = -\alpha_-$, then $\beta_0 = \alpha_+$, even though $\alpha_0 = 0$; while if the flow in the lower-half space is irrotational and $\alpha_- = 0$, then $\beta_0 = \alpha_+/\sqrt{2}$ and $\alpha_0 = \alpha_+/2$.

B.1 Formulation

Consider a velocity perturbation (u, v) of an unperturbed shear flow $(\alpha y, 0)$, where (x, y) are spatial coordinates and α is a constant shear rate. The two-dimensional incompressible Euler equations for (u, v) and the pressure p are

$$\begin{aligned} u_t + (\alpha y + u) u_x + v(\alpha + u_y) + p_x &= 0, \\ v_t + (\alpha y + u) v_x + v v_y + p_y &= 0, \\ u_x + v_y &= 0. \end{aligned}$$

Since the vorticity is advected by the perturbed flow, and the unperturbed vorticity is constant (equal to $-\alpha$), it is consistent to assume that the flow perturbations are irrotational.

We therefore introduce a velocity potential $\phi(x, y, t)$ such that

$$u = \phi_x, \quad v = \phi_y$$

and a streamfunction $\psi(x, y, t)$ such that

$$u = \psi_y, \quad v = -\psi_x.$$

Then the incompressibility condition implies that

$$(B.6) \quad \Delta\phi = 0,$$

and an integration of the momentum equations gives

$$(B.7) \quad \phi_t + \alpha(y\phi_x - \psi) + \frac{1}{2}|\nabla\phi|^2 + p = 0.$$

Next, we consider perturbations of a shear flow given by $(\alpha_+y, 0)$ in $y > 0$ and $(\alpha_-y, 0)$ in $y < 0$, where the shear rates α_{\pm} are distinct constants. The unperturbed flow has a jump in vorticity across $y = 0$. We assume that the flow perturbations are irrotational, and that the interface is a graph. We write the perturbed location of the interface where the vorticity jumps as

$$y = \eta(x, t).$$

We use the notation

$$(B.8) \quad \alpha = \begin{cases} \alpha_+ & \text{if } y > \eta(x, t), \\ \alpha_- & \text{if } y < \eta(x, t), \end{cases}$$

with similar notation for other quantities that jump across the interface.

The kinematic boundary condition states that the interface moves with the fluid, meaning that

$$(B.9) \quad \eta_t + (\alpha\eta + \phi_x)\eta_x - \phi_y = 0 \quad \text{on } y = \eta(x, t)^{\pm}.$$

The dynamic boundary condition states that the pressure is continuous across the interface, meaning that

$$(B.10) \quad [p] = 0,$$

where

$$[f](x, t) = f(x, \eta(x, t)^+, t) - f(x, \eta(x, t)^-, t)$$

denotes the jump in a quantity $f(x, y, t)$ across $y = \eta(x, t)$. Using (B.7) in (B.10), we get

$$(B.11) \quad \left[\phi_t + \alpha(y\phi_x - \psi) + \frac{1}{2}|\nabla\phi|^2 \right] = 0.$$

Finally, we require that the flow perturbation and the pressure decay to zero away from the interface. This condition, together with (B.6), gives

$$(B.12) \quad \begin{aligned} \Delta\phi &= 0 && \text{in } y > \eta(x, t), y < \eta(x, t), \\ \phi(x, y, t) &\rightarrow 0 && \text{as } y \rightarrow \pm\infty. \end{aligned}$$

The full set of equations consists of (B.9), (B.11), and (B.12), where ψ is the harmonic conjugate of ϕ such that $\psi \rightarrow 0$ as $y \rightarrow \pm\infty$.

B.2 Linearized equations

Linearizing (B.9), (B.11), and (B.12) around the unperturbed solution $\phi = 0$, $\eta = 0$, we get

$$\begin{aligned}\Delta\phi &= 0 && \text{in } y > 0 \text{ and } y < 0, \\ \eta_t - \phi_y &= 0 && \text{on } y = 0^\pm, \\ [\phi_t - \alpha\psi] &= 0, \\ \phi(x, y, t) &\rightarrow 0 && \text{as } |y| \rightarrow \infty,\end{aligned}$$

where $[\cdot]$ now denotes a jump across $y = 0$. Taking the jump of the kinematic boundary condition $\eta_t - \phi_y = 0$ across $y = 0$, we get

$$[\phi_y] = 0.$$

A Fourier solution of $\Delta\phi = 0$ that decays as $|y| \rightarrow \infty$ has the form

$$\phi(x, y, t) = \begin{cases} \hat{A}_+(k)e^{ikx - |k|y - i\omega t} & \text{in } y > 0, \\ \hat{A}_-(k)e^{ikx + |k|y - i\omega t} & \text{in } y < 0, \end{cases}$$

where $k \in \mathbb{R}$. We write this as

$$\phi(x, y, t) = \hat{A}(k)e^{ikx - \sigma|k|y - i\omega t},$$

where $\hat{A} = \hat{A}_\pm$, and

$$\sigma = \begin{cases} +1 & \text{if } y > 0, \\ -1 & \text{if } y < 0. \end{cases}$$

The corresponding streamfunction and interface displacement are

$$\psi(x, y, t) = \hat{B}(k)e^{ikx - \sigma|k|y - i\omega t}, \quad \eta(x, t) = \hat{F}(k)e^{ikx - i\omega t},$$

where

$$(B.13) \quad \hat{A}(k) = i\sigma \operatorname{sgn}(k)\hat{B}(k), \quad \hat{F}(k) = \frac{k}{\omega}\hat{B}(k).$$

Using these solutions in the jump conditions and eliminating \hat{A} , we find that

$$[\{\sigma\omega \operatorname{sgn}(k) - \alpha\}\hat{B}] = 0, \quad [\hat{B}] = 0.$$

It follows that \hat{B} is continuous across $y = 0$, and

$$(B.14) \quad \omega = \omega_0 \operatorname{sgn}(k)$$

where the frequency ω_0 is given in (B.3).

Superposing Fourier solutions, we get the linearized solution with general spatial dependence,

$$\begin{aligned}\phi(x, y, t) &= A(x, y)e^{-i\omega_0 t} + A^*(x, y)e^{i\omega_0 t} \\ \psi(x, y, t) &= B(x, y)e^{-i\omega_0 t} + B^*(x, y)e^{i\omega_0 t}, \\ \eta(x, t) &= F(x)e^{-i\omega_0 t} + F^*(x)e^{i\omega_0 t}.\end{aligned}$$

Here, the complex amplitudes A , B , F consist of positive wavenumbers,

$$\begin{aligned} A(x, y) &= \int_0^\infty \hat{A}(k) e^{ikx - \sigma ky} dk, \\ B(x, y) &= \int_0^\infty \hat{B}(k) e^{ikx - \sigma ky} dk, \\ F(x) &= \int_0^\infty \hat{F}(k) e^{ikx} dk, \end{aligned}$$

and, from (B.13),

$$A(x, y) = i \operatorname{sgn}(y) B(x, y), \quad F(x) = \frac{i}{\omega_0} B_x(x, 0).$$

We remark that the linearized tangential fluid velocity U on the interface is the sum of the x -velocity components of the unperturbed shear flow and the flow perturbation, so

$$U = \alpha \eta + \phi_x|_{y=0}.$$

We compute from the linearized solution that U is continuous across the interface, as it must be, and is given by

$$(B.15) \quad U(x, t) = \alpha_0 \eta(x, t)$$

where α_0 is defined in (B.5). Thus, since $\eta(x, t)$ has zero mean with respect to t , the time-averaged translation of the interface in the x -direction is zero according to the linearized theory. In the symmetric case $\alpha_0 = 0$, the linearized x -velocity is identically zero. In the general case, the advection of the interface in one direction for positive displacements is canceled by its advection in the opposite direction for negative displacements. There is, however, a nonlinear Stokes drift of the interface that is second-order in the amplitude.

For use in the asymptotic expansion, we state a solvability condition for the nonhomogeneous linearized problem,

$$(B.16) \quad \begin{aligned} \Delta \phi &= 0 && \text{in } y > 0 \text{ and } y < 0, \\ [\phi_y] &= f(x) e^{-in\omega_0 t} && \text{on } y = 0, \\ [\phi_t - \alpha \psi] &= g(x) e^{-in\omega_0 t} && \text{on } y = 0, \\ \phi(x, y, t) &\rightarrow 0 && \text{as } |y| \rightarrow \infty. \end{aligned}$$

Proposition B.1. *If $n^2 \neq 1$, then (B.16) is solvable for ϕ for any functions $f, g \in L^2(\mathbb{R})$. If $n = 1$, then (B.16) is solvable if and only if*

$$(B.17) \quad \mathbf{P}[\alpha_0 f + g] = 0,$$

where α_0 is defined in (B.5) and \mathbf{P} is defined in (1.4).

Proof. Write $\phi(x, y, t) = \Phi(x, y) e^{-in\omega_0 t}$, take the Fourier transform of (B.16) with respect to x , and solve the resulting equations. The details are omitted. \square

B.3 Weakly nonlinear solution

We look for an asymptotic solution of (B.9), (B.11), and (B.12), depending on a small parameter ε , of the form

$$\begin{aligned}\phi^\varepsilon(x, y, t) &= \varepsilon\phi_1(x, y, \varepsilon^2 t, t) + \varepsilon^2\phi_2(x, y, \varepsilon^2 t, t) + \varepsilon^3\phi_3(x, y, \varepsilon^2 t, t) + \dots, \\ \psi^\varepsilon(x, y, t) &= \varepsilon\psi_1(x, y, \varepsilon^2 t, t) + \varepsilon^2\psi_2(x, y, \varepsilon^2 t, t) + \varepsilon^3\psi_3(x, y, \varepsilon^2 t, t) + \dots, \\ \eta^\varepsilon(x, t) &= \varepsilon\eta_1(x, \varepsilon^2 t, t) + \varepsilon^2\eta_2(x, \varepsilon^2 t, t) + \varepsilon^3\eta_3(x, \varepsilon^2 t, t) + \dots\end{aligned}$$

The velocity potentials ϕ_n and streamfunctions ψ_n satisfy

$$\Delta\phi_n = 0, \quad \psi_{ny} = \phi_{nx}, \quad \psi_{nx} = -\phi_{ny}.$$

Expansion and simplification of the boundary conditions yields the following perturbation equations: at the order ε ,

$$\begin{aligned}\eta_{1t} - \phi_{1y} &= 0, \\ [\phi_{1t} - \alpha\psi_1] &= 0;\end{aligned}$$

at the order ε^2 ,

$$\begin{aligned}\eta_{2t} - \phi_{2y} + \alpha\eta_1\eta_{1x} + \eta_{1x}\phi_{1x} - \eta_1\phi_{1yy} &= 0, \\ \left[\phi_{2t} - \alpha\psi_2 + \eta_1\phi_{1ty} + \frac{1}{2}|\nabla\phi_1|^2\right] &= 0;\end{aligned}$$

and, at the order ε^3 ,

$$\begin{aligned}\eta_{3t} - \phi_{3y} + \eta_1\tau + \alpha(\eta_1\eta_{2x} + \eta_2\eta_{1x}) + \eta_{1x}\phi_{2x} + \eta_{2x}\phi_{1x} + \eta_1\eta_{1x}\phi_{1xy} \\ - \eta_1\phi_{2yy} - \eta_2\phi_{1yy} - \frac{1}{2}\eta_1^2\phi_{1yyy} &= 0, \\ \left[\phi_{3t} - \alpha\psi_3 + \phi_{1\tau} + \eta_2\phi_{1ty} + \eta_1\phi_{2ty} + \frac{1}{2}\eta_1^2\phi_{1tyy} \right. \\ \left. - \frac{1}{2}\alpha\eta_1^2\psi_{1xx} + \nabla\phi_1 \cdot \nabla\phi_2 + \eta_1\nabla\phi_1 \cdot \nabla\phi_{1y}\right] &= 0.\end{aligned}$$

Here, all boundary conditions and jumps are evaluated at $y = 0$.

The solution of the first-order equations is

$$\begin{aligned}\phi_1(x, y, \tau, t) &= A(x, y, \tau)e^{-i\omega_0 t} + A^*(x, y, \tau)e^{i\omega_0 t}, \\ \psi_1(x, y, \tau, t) &= B(x, y, \tau)e^{-i\omega_0 t} + B^*(x, y, \tau)e^{i\omega_0 t}, \\ \eta_1(x, \tau, t) &= F(x, \tau)e^{-i\omega_0 t} + F^*(x, \tau)e^{i\omega_0 t},\end{aligned}$$

where $B(x, y, \tau)$ is continuous across $y = 0$ with $\mathbf{P}[B(x, 0, \tau)] = 0$, and

$$A(x, y, \tau) = i\sigma B(x, y, \tau), \quad F(x, \tau) = -\frac{i}{\omega_0}B_x(x, 0, \tau).$$

Using these expressions in the second-order equations and solving the result, we find that

$$\begin{aligned}\phi_2(x, y, \tau, t) &= C(x, y, \tau)e^{-2i\omega_0 t} + M(x, y, \tau) + C^*(x, y, \tau)e^{2i\omega_0 t}, \\ \psi_2(x, y, \tau, t) &= D(x, y, \tau)e^{-2i\omega_0 t} + N(x, y, \tau) + D^*(x, y, \tau)e^{2i\omega_0 t}, \\ \eta_2(x, \tau, t) &= G(x, \tau)e^{-2i\omega_0 t} + G^*(x, y, \tau)e^{2i\omega_0 t},\end{aligned}$$

where

$$\begin{aligned}D(x, y, \tau) &= -\frac{\alpha}{2\omega_0^2} B_x^2(x, y, \tau), \\ N(x, y, \tau) &= -\frac{\beta}{\omega_0^2} B_x(x, y, \tau) B_x^*(x, y, \tau) \\ G(x, \tau) &= \frac{i\alpha_0}{2\omega_0^3} \{B_x^2(x, 0, \tau)\}_x,\end{aligned}$$

with

$$\beta = \begin{cases} \alpha_- & \text{if } y > 0, \\ \alpha_+ & \text{if } y < 0, \end{cases} \quad C = i\sigma D, \quad M_x = N_y, \quad M_y = -N_x.$$

We use these expression in the third-order equations, collect terms proportional to $e^{-i\omega_0 t}$, and impose the solvability condition (B.17). After writing this condition in terms of F and simplifying the result, we find that $F(x, \tau)$ satisfies (B.2).

Acknowledgment.

JB was partially supported by the NSF under grant number DMS-0604947. JKH was partially supported by the NSF under grant number DMS-0607355.

Bibliography

- [1] Ali, G.; Hunter, J. K. Nonlinear surface waves on a tangential discontinuity in magnetohydrodynamics. *Quart. Appl. Math* **61** (2003), no. 3, 451–474.
- [2] Ali, G.; Hunter, J. K.; Parker, D. Hamiltonian equations for scale invariant waves. *Stud. Appl. Math.* **108** (2002), no. 3, 305–321.
- [3] Chemin, J.-Y. Two-dimensional Euler system and the vortex patches problem. *Handbook of Mathematical Fluid Dynamics*, Vol. III, ed. S. Friedlander and D. Serre, Elsevier, 2004.
- [4] Constantin, P.; Lax, P.; Majda, A. J. A simple one-dimensional model for the three-dimensional vorticity equation. *Comm. Pure Appl. Math.* **104** (1986), no. 6, 603–616.
- [5] Dritschel, D. G. The repeated filamentation of two-dimensional vorticity interfaces. *J. Fluid Mech.* **194** (1988), 511–547.
- [6] M. F. Hamilton, Yu. A. Illinsky, and E. A. Zabolotskaya, Evolution equations for nonlinear Rayleigh waves, *J. Acoust. Soc. Amer.* **97** (1995), no. 2, 891–897.
- [7] J. K. Hunter, Asymptotic equations for nonlinear hyperbolic waves, in *Surveys in Applied Mathematics*, Vol 2, ed. M Freidlin et. al., Plenum Press, New York, 1995.
- [8] H. Liu, Wave breaking in a class of nonlocal dispersive wave equations, *J. Nonlinear Math. Phys.* **13** (2006), no. 3, 441–466.
- [9] A. J. Majda and A. L. Bertozzi, *Vorticity and Incompressible Flow*, Cambridge University Press, Cambridge, 2002.

- [10] J. Marsden and A. Weinstein, Coadjoint orbits, vortices, and Clebsch variables for incompressible fluids, *Physica D* **7** (1983), nos. 1–3, 305–323.
- [11] P. G. Saffman, *Vortex Dynamics*, Cambridge University Press, Cambridge, 1992.
- [12] Whitham, G. B. *Linear and Nonlinear Waves*. John Wiley & Sons, New York, 1974.
- [13] V. E. Zakharov, V. S. Lvov, and G. Falkovich, *Kolmogorov Spectra of Turbulence I*, Springer-Verlag, Berlin, 1992.

Received Month 200X.